THE JOURNAL OF BIOLOGICAL CHEMISTRY VOL. 286, NO. 18, pp. 15862–15874, May 6, 2011

CD44v6 Coordinates Tumor Matrix-triggered Motility and Apoptosis Resistance*[S]

Received for publication, December 1, 2010, and in revised form, February 1, 2011 Published, JBC Papers in Press, March 3, 2011, DOI 10.1074/jbc.M110.208421

Thorsten Jung[‡], Wolfgang Gross[§], and Margot Zöller[‡¶1]

From the Departments of [‡]Tumor Cell Biology, University Hospital of Surgery, and [§]Experimental Surgery, University of Heidelberg, D-69120 Heidelberg, Germany and [¶]German Cancer Research Center, D-69120 Heidelberg, Germany

Tumor progression requires a crosstalk with the tumor surrounding, where the tumor matrix plays an essential role. We recently reported that only the matrix delivered by a CD44v6-competent (ASML^{wt}), but not that of a CD44v6-deficient (ASML-CD44v^{kd}) rat pancreatic adenocarcinoma line supports metastasis formation. We here describe that this matrix provides an important feedback toward the tumor cell and that CD44v6 accounts for orchestrating signals received from the matrix. ASML^{wt} cells contain more hyaluronan synthase-3 and secrete higher amounts of >50 kDa HA than ASML-CD44v^{kd} cells, which secrete more hyaluronidase. Only the ASML^{wt}-matrix supports migration and apoptosis resistance, which both can be initiated via CD44v6, c-Met, and $\alpha 6\beta 4$ ligand binding and proceed via FAK, PI3K/Akt, and MAPK activation, respectively. However, c-Met- and $\alpha 6\beta 4$-initiated signaling are strongly augmented by the association with CD44v6 as only very weak effects are observed in CD44v6-deficient cells. The same CD44v6-dependent convergence of motility- and apoptosis resistance-related signals also accounts for human tumor lines. Thus, CD44v6 promotes motility and apoptosis resistance via its involvement in assembling a matrix that, in turn, triggers activation of signaling cascades, which proceeds, independent of the initiating receptor-ligand interaction, in a concerted action via CD44v6.

Tumor cells require a special surrounding for survival and metastatic progression (1, 2). Tumor cells support this crosstalk with the host by secreting and assembling a tumor matrix (3, 4). One of the molecules that has been amply demonstrated to contribute to the metastatic process is CD44 (5, 6), particularly the CD44 variant isoform v6 (CD44v6)[2] (7, 8). In fact, this multifaceted molecule encompasses many activities facilitating the metastatic process.

First, the most important feature of CD44 in the communication with the tumor surrounding is its quality as the major hyaluronan (HA) receptor (9, 10). By HA binding, the CD44 conformation becomes altered such that its cytoplasmic tail interacts with the cytoskeleton via ankyrin (11) and ERM (Ezrin/Radixin/Moesin) proteins (12), which guide CD44 to the leading edge of migrating cells (13). The CD44-HA interaction also stimulates MMP2 and MMP9 production (14) and promotes MMP9 binding to CD44, which supports invasiveness by focalized matrix degradation (14). HA also binds to endothelial cells through CD44. Proinflammatory cytokines stimulate CD44 expression and strengthens endothelial cell HA binding (15). This, in turn facilitates tumor cell attachment via CD44, rolling and finally extravasation (16).

Second, besides binding to HA, CD44 also acts as a receptor for several cytokines and chemokines deposited in the extracellular matrix (ECM) (17–19), which trigger activation of signal transduction cascades (5, 6, 8). CD44 itself does not display kinase activity. Instead it initiates signal transduction via associated receptor tyrosine kinases (RTK) (20–24), or via interaction of the cytoplasmic tail with non-RTK and linker proteins (6, 25). Thus, CD44 co-immunoprecipitates with all ERBB RTK family members. To give an example, the CD44-HA interaction initiates ERBB2 phosphorylation and stimulation of HA production induces assembly of a lipid raft integrated complex of ERBB2, CD44, ezrin, the chaperone molecules HSP90 and CDC37 and PI3K, where activation of the PI3K/Akt pathway promotes apoptosis resistance (25). HER4 activation also proceeds via CD44, where CD44 heparan sulfate side chain-bound MMP7 cleaves heparin binding growth factor, a prerequisite for HER4 activation (26). Another important CD44 partner in apoptosis protection is c-Met. CD44 promotes c-Met phosphorylation via CD44v3- or CD44v6-bound hepatocyte growth factor (HGF). For not yet defined reasons, c-Met activation via CD44 requires the cytoplasmic tail of CD44 and the interaction with ERM proteins for activation of the Ras-MAPK pathway (27, 28). The most important CD44-associated non-RTK are members of the src family (29). As membrane-attached molecular switch, src has a central role by linking a variety of extracellular signals to crucial intracellular signaling pathways (30). Essential for their association with CD44 is the membrane subdomain location. Both CD44 and non-RTK are located in glycolipid-enriched membrane microdomains (GEM) that are prone for collecting signal transducing and linker molecules (6).

Third, there is strong evidence that CD44 is involved in the assembly of the matrix (31–33) such that the HA-CD44 association modifies the tissue matrix to support colonization (34, 35). Perturbation in matrix components can alter intracellular tension resulting in shifts in signaling events that affect gene

* This work was supported by the DFG/SPP1190 and NCT (to M. Z.).
[S] The on-line version of this article (available at http://www.jbc.org) contains supplemental Tables S1–S3 and Figures S1–S4.
[1] To whom correspondence should be addressed: Department of Tumor Cell Biology, University Hospital of Surgery, Im Neuenheimer Feld 365, D-69120 Heidelberg, Germany. Tel.: 06221-565146; Fax: 06221-565199; E-mail: margot.zoeller@uni-heidelberg.de.
[2] The abbreviations used are: CD44v, CD44 variant isoforms; AS, BSp73AS; ASML, BSp73ASML; ECM, extracellular matrix; ERM, ezrin, radixin, moesin; GEM, glycolipid-enriched membrane microdomain; HA, hyaluronan; HAase, hyaluronidase; HAS3, hyaluronan synthase-3; HGF, hepatocyte growth factor; kd, knockdown; LN5, laminin 5; RTK, receptor tyrosine kinase; WB, Western blot.

expression (36). By its nature as a transmembrane proteoglycan CD44 allows the local concentration of glycosaminoglycan-associating proteins that frequently lowers the threshold for signal transduction (37), where binding of osteopontin, bFGF, VEGF, and HGF are of special interest for the metastatic process (38–41). We recently reported that a CD44v knockdown (kd) in a highly metastatic tumor line (ASML) (42) revealed a striking reduction in metastatic capacity, which was, at least in part, due to an altered tumor matrix. The CD44v^{kd}, distinct to CD44v-competent cells secrete a matrix that does not support adhesion of CD44v^{wt} or CD44v^{kd} cells, whereas both cells readily adhere to the CD44v^{wt}-matrix (43, 44).

Based on these latter findings, we searched for additional differences in the matrix assembled by CD44v-competent *versus* CD44v-deficient cells and asked, whether the feedback from the tumor matrix can account for the striking loss in metastatic capacity of ASML-v4–7^{kd} cells. We show for human and rat pancreatic adenocarcinoma cells that only a matrix derived from CD44v6-competent cells supports tumor cell migration and apoptosis resistance. Furthermore, matrix-, as well as HA- or HGF- or laminin5 (LN5)-initiated activation of CD44v6, c-Met, and $\alpha6\beta4$ essentially requires coordination via CD44v6.

EXPERIMENTAL PROCEDURES

Tumor Lines—ASML^{wt}, ASML-v4–7^{kd}, AS, AS-v6, and AS-v4–7 clones of a BDX pancreatic adenocarcinoma (7, 42, 43, 45) were maintained in RPMI 1640/10% FCS. The level of panCD44, CD44s, and CD44v6 expression is shown in supplemental Fig. S1. c-Met-, $\beta4$-, and CD44v6-siRNA transfection followed the supplier's suggestion (Qiagen, Hildesheim, Germany). Efficiency of silencing was monitored after 48 h by Western blot (WB). Central features of these lines and of the human pancreatic adenocarcinoma lines Capan2, 8.18, and Pt45P1 are listed in supplemental Table S1.

Antibodies—Primary antibodies are listed in supplemental Table S2. Streptavidin-HRP and dye-labeled secondary antibodies were obtained commercially.

Inhibitors—LY294002 (PI3K-inhibitor) (Calbiochem, Darmstadt, Germany), SU11274 (c-Met-inhibitor), and GW5074 (raf-inhibitor) (Sigma, Munich, Germany) were used as indicated.

Cell and Conditioned Medium Fractionation—For cytosol preparation, 2.5×10^6 cells were incubated in hypotonic buffer, homogenized, and centrifuged ($800 \times g$) to pellet nuclei. After adding Nonidet-P40 (0.5%), vortexing and centrifugation ($1600 \times g$, 5 min), cytosolic proteins were recovered from the supernatant. Conditioned medium, derived from tumor cells cultured for 48 h in serum-free medium, was centrifuged (10 min, $1000 \times g$, 10 min $1500 \times g$, 10 min $2000 \times g$, 20 min $10{,}000 \times g$, 90 min $26{,}000 \times g$). This vesicle-depleted supernatant, termed "matrix," was used throughout.

In Vitro Kinase Assay—Immune complexes were suspended in lysis buffer containing a protease inhibitor mix (Roche, Mannheim, Germany). After centrifugation, beads were resuspended in 30 μl of kinase assay buffer, 10 μCi of [γ-^{32}P]ATP and incubated (15 min, 37 °C). The reaction was stopped by adding 10 μl of non-reducing 6× Laemmli buffer. SDS-PAGE was followed by autoradiography.

Immunoprecipitation—Cells were washed in HEPES buffer and lysed (30 min, 4 °C, HEPES buffer, 1% Lubrol, 1 mM PMSF, 1 mM $NaVO_4$, 10 mM NaF, protease inhibitor mix). Centrifuged lysates, mixed with the antibody, were immunoprecipitated and incubated with Protein G-Sepharose. Immune complexes were washed, dissolved in Laemmli buffer, and resolved by SDS-PAGE.

SDS-PAGE and WB—SDS-PAGE resolved proteins were transferred (nitrocellulose membranes), membranes were blocked, blotted with primary and HRP-conjugated secondary antibodies and developed with the ECL kit. For MALDI-TOF analysis, proteins were separated by two-dimensional gel analysis and silver-stained.

MALDI-TOF Mass Spectrometry—Silver-stained spots were excised. Protein digestion, sample preparation, MALDI-TOF fingerprint analysis, post-source-decay fragmentation analysis, and database searches are described (46).

Flow Cytometry—Cells (2×10^5) were stained with AnnexinV-APC/PI. Samples were processed in a FACS-Calibur with the CellQuest program (BD, Heidelberg, Germany).

Immunofluorescence—Cells on coverslides were fixed, permeabilized, blocked, incubated with primary antibodies, fluorochrome-conjugated secondary antibodies, blocked, incubated with second, dye-labeled antibodies or with a second antibody followed by a dye-labeled secondary antibody and washed. Coverslides were mounted in Elvanol. Digitized images were generated using a 40× objective (Leica DMRBE microscope, SPOT-CCD camera, Diagnostic Instruments, Software SPOT2.1.2). Overlays of single fluorescence are shown.

ELISA—96-well plates were coated at pH 7.2 with matrix or HA. After washing, HA was determined using biotinylated HA-binding protein and streptavidin-biotin for detection. Hyaluronidase (HAase) levels were measured according to Stern and Stern (47). HAase concentrations (mU/ml) were determined by hyaluronidase dilution curves.

Apoptosis Induction—Cells (1×10^5) were grown for 48 h in RPMI/10% FCS containing serial dilutions of cisplatin (Sigma). Survival was monitored by annexinV-APC/PI staining, MTT assay, and [^{3}H]thymidine uptake.

Migration—Cells, in the upper part of a Boyden chamber (40 μl of RPMI/0.1% BSA), were separated from the lower part, containing 30 μl of RPMI/1% FCS, 20% FCS, 5 ng/ml HGF, 10 μg/ml HA, 2 μg/ml LN5, ASML^{wt}-, or ASML-v4–7^{kd}-matrix, by a 8-μm pore size polycarbonate-membrane (Neuroprobe, Gaithersburg, MD). Where indicated, the ASML^{wt} matrix was treated for 2 h with 0.5 mg/ml HAase type IV-S (Sigma) or the ASML-v4–7^{kd} matrix was supplemented with HA (10 μg/ml). Migration was evaluated after 16 h by lower membrane side staining with crystal-violet. After lysis, A_{595} nm was measured. Migration is presented as % of input cells.

Video Microscopy—Hoechst 33342-stained cells (5×10^4) were seeded on matrix-coated migration chambers (8-well μ-slides, ibidi, Martinsried, Germany). Chambers were placed under an Olympus IX81 inverse microscope with a Hg/Xe lamp, an incubation chamber (37 °C, 5%CO_2), a CCD camera (Hamamatsu), and a ScanR acquisition software (Olympus, Hamburg, Germany). Two pictures (20-fold magnification)/chamber (2ms exposure) were taken every 15 min for 12 h.

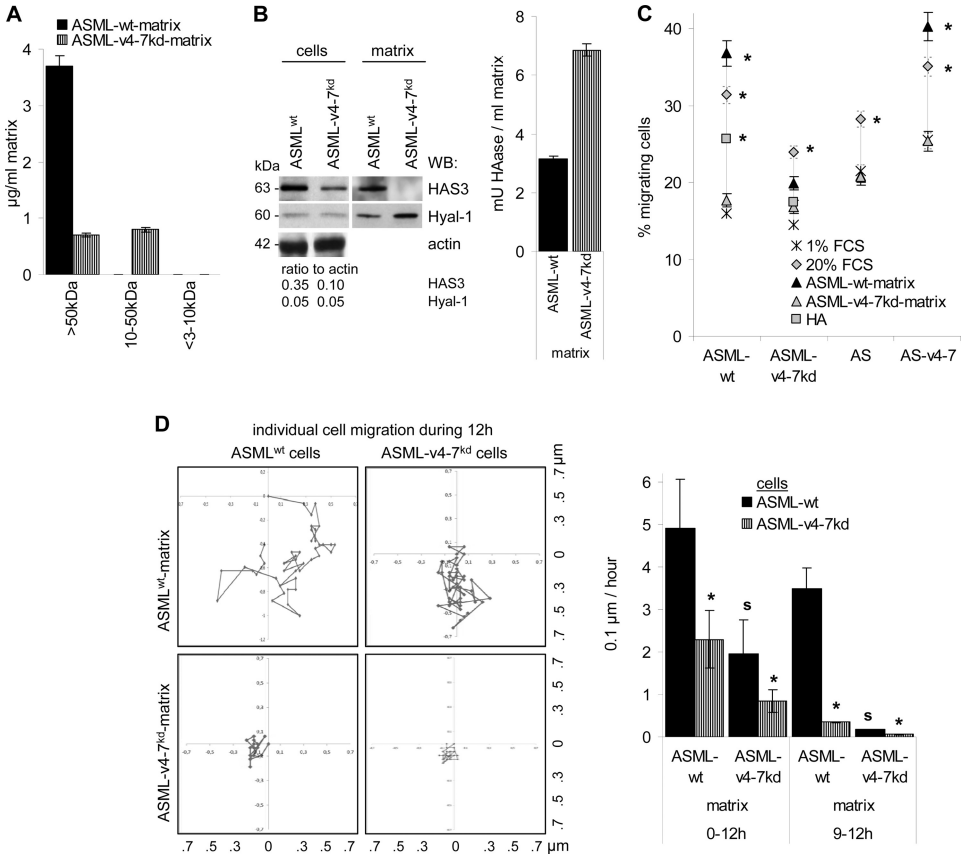

FIGURE 1. **Recovery of HA in the ASML^{wt}-matrix and tumor cell migration.** *A*, ASML^{wt}- and the ASML-v4–7^{kd}-matrix were fractionated by filtration through 3000, 10,000, and 50,000 MW pore size filters and titrated amounts of the size-separated matrix or HA (1–20 μg/ml) were seeded on ELISA plates and recovery of HA in the ASML^{wt}- and the ASML-v4–7^{kd}-matrix was determined with biotinylated HA-binding protein and streptavidin-biotin. Mean ± S.D. of triplicates is shown. *B*, WB of Hyal-1 and HAS3 in ASML^{wt} and ASML-v4–7^{kd} cell lysates and the matrix. Gels were loaded with 25 μg of lysate. For the quantification of HAase, titrated amounts of matrix or HAase (0–25mU/ml) were seeded on ELISA plates coated with 200 μg/ml HA. After 16 h of incubation, plates were washed and remaining HA was determined as above. HAase concentrations (mU/ml) were calculated according to standard HAase dilution curves. *C*, migration of AS, AS-v4–7, ASML^{wt}, and ASML-v4–7^{kd} cells toward FCS, HA, the ASML^{wt}- and the ASML-v4–7^{kd}-matrix (Boyden chamber). The percentage of migrating cells was determined after 18 h. Mean ± S.D. of triplicates are shown. Significant differences between ASML^{wt} and ASML-v4–7^{kd} cells are indicated by *. *D*, migration of ASML^{wt} and ASML-v4–7^{kd} cells on the ASML^{wt}- and the ASML-v4–7^{kd}-matrix as revealed by video microscopy. Pictures were taken every 15 min. The movement of individual cells during 12 h and the mean movement per hour ± S.D. of 20 cells during 0–12 h and during 9–12 h after seeding are shown. Significant differences in cell motility on the ASML^{wt} *versus* the ASML-v4–7^{kd} matrix are indicated by **s**; significant differences in the motility of ASML^{wt} *versus* ASML-v4–7^{kd} cells are indicated by *. The ASML^{wt} matrix strongly promotes motility of ASML^{wt} cells, but has only a weak and transient effect on ASML-v4–7^{kd} cell motility.

Migration was quantified according to Manual_tracking plugin (F.P. Cordeliére, Centre de Recherche de l'Institute Curie) running in the open-source software Image J (NIH). Path length of 20 individual cells in each setting was calculated for every 15 min by customized programs. The mean pathway length per 1 h during the incubation period of 0–12 h and of 9–12 h is presented.

Statistics—Significance of triplicates or of 20 individual values was calculated by Student's *t* test. Assays were repeated three times.

RESULTS

Highly metastatic CD44v6-competent ASML^{wt} cells assemble a matrix, which supports metastasis formation (44). This finding suggests a feedback trigger from the matrix toward the tumor cell. The hypothesis and the involvement of CD44v6 was controlled for two most characteristic features of metastasizing tumor cells, motility, and apoptosis resistance.

CD44v6 and Matrix-supported Motility—The ASML^{wt}-matrix contains, besides others, higher amounts of HGF, c-Met, uPA, uPAR, MMP2, and MMP9 (44, supplemental Table S3) that might support cell motility. In addition, compared with the ASML-v4–7^{kd}-matrix, the ASML^{wt}-matrix is enriched in >50 kDa HA (Fig. 1*A*). ASML^{wt} cells and the matrix contain higher amounts of hyaluronan synthase-3 (HAS3). The ASML-v4–7^{kd}-matrix, instead, contains a higher amount of HAase (Fig. 1*B*). These differences have significant bearing on cell motility. The ASML^{wt}-, but not the ASML-v4–7^{kd}-matrix promotes transwell migration of CD44v6-expressing cells (Fig. 1*C*). Time lapse video microscopy for 12 h revealed migration of ASML^{wt} cells on the ASML^{wt}-, but not the ASML-v4–7^{kd}-matrix. ASML-v4–7^{kd} cells did not migrate on their own matrix. They showed some migratory activity on the ASML^{wt}-matrix in the starting hours. However, their migratory activity rapidly declined and during the last 4 h of culture ASML-v4–7^{kd} cells no longer moved at all (Fig. 1*D*).

To control whether CD44v6 contributes to the response toward the ASML^{wt}-matrix, migration (Boyden chamber) was evaluated after pre-incubation of ASML^{wt} (CD44s$^+$/CD44v$^+$/c-Met$^+$/α6β4$^+$), ASML-v4–7^{kd} (CD44s$^+$/CD44v4–7$^-$/c-Met$^+$/α6β4$^+$), ASML-v6^{kd} (CD44s$^+$/CD44v6$^-$/c-Met$^+$/α6β4$^+$), AS

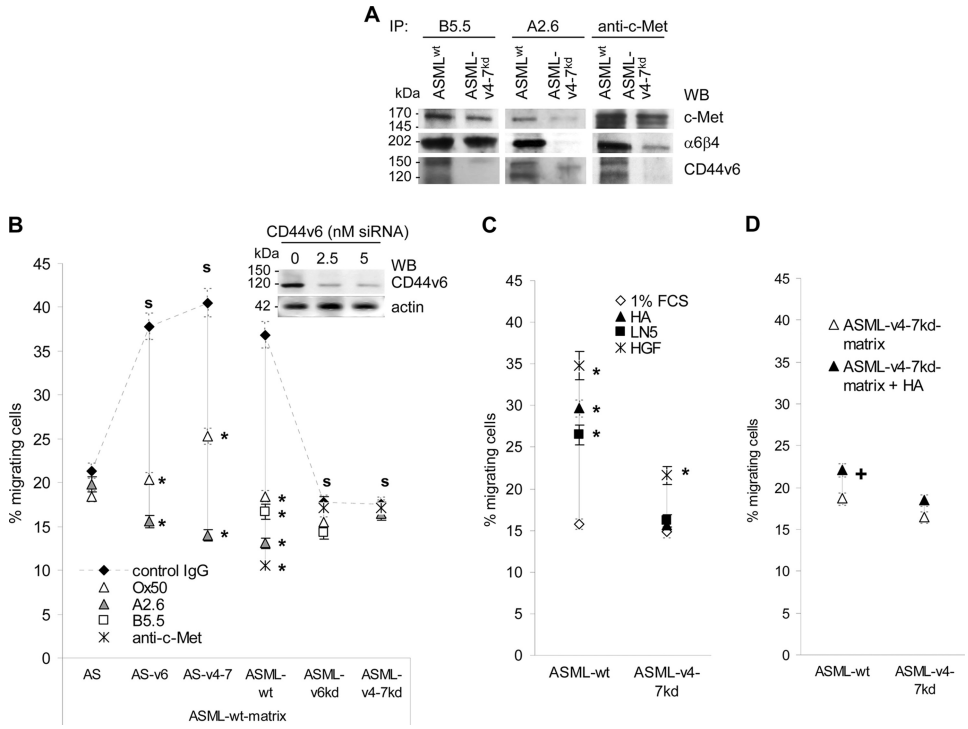

FIGURE 2. **The contribution of CD44v6, c-Met, and α6β4 to ASML^{wt} cell migration.** *A*, ASML^{wt} and ASML-v4–7^{kd} lysates from 10^7 cells were immunoprecipitated with B5.5 (anti-α6β4), anti-c-Met, and A2.6 (anti-CD44v6). Immunoprecipitates were separated by SDS-PAGE and after transfer blotted with anti-c-Met, B5.5, and A2.6. CD44v6, c-Met and α6β4 co-immunoprecipitate. *B*, ASML^{wt}, ASML-v4–7^{kd}, ASML-v6^{kd}, AS, AS-v4–7, and AS-v6 cells were pre-incubated with Ox50 (anti-panCD44), A2.6, B5.5, and anti-c-Met. Migration toward the ASML^{wt} matrix was evaluated. *C*, migration of ASML^{wt} and ASML-v4–7^{kd} cells toward HA, LN5 and HGF was evaluated. *D*, migration of ASML^{wt} and ASML-v4–7^{kd} cells toward the ASML-v4–7^{kd}-matrix with/without addition of 10 μg/ml HA was evaluated. *B–D*, the percentage of migrating cells (Boyden chamber) was determined after 18 h. Mean ± S.D. of triplicates are shown. Significant inhibition by antibody pre-incubation is indicated by *. Significant differences in dependence on CD44v6 expression is indicated by **s**. Significant differences by HA addition is indicated by **+**. The ASML^{wt}-matrix, but also HA, LN5 and HFG promote ASML^{wt} cell migration and anti-CD44v6, -c-Met, or -α6β4 inhibit ASML^{wt} cell migration. Thus, CD44v6, c-Met, and α6β4 jointly promote ASML^{wt} cell migration. However, anti-CD44v6 only inhibits migration of AS-v4–7, AS-v6, and ASML^{wt} cells. On the contrary, anti-panCD44 does not inhibit migration of CD44v6-deficient AS, ASML-v4–7^{kd}, and ASML-v6^{kd} cells, which implies that migration-promoting activity of CD44, c-Met, and α6β4 is coordinated by CD44v6.

(CD44s$^+$/CD44v$^-$/c-Met$^+$/α6β4$^-$), AS-v6 (CD44s$^+$/CD44v6$^+$/c-Met$^+$/α6β4$^-$), and AS-v4–7 (CD44s$^+$/CD44v4–7$^+$/c-Met$^+$/α6β4$^-$) cells with anti-panCD44 (Ox50), anti-CD44v6 (A2.6), anti-c-Met, and anti-α6β4 (B5.5). The latter two antibodies have been included, because α6β4 and c-Met co-immunoprecipitate with CD44v6 and c-Met co-immunoprecipitates with α6β4 (27, 48) (Fig. 2*A*). Pre-incubation with anti-panCD44, anti-CD44v6, anti-c-Met, and anti-α6β4 significantly inhibited ASML^{wt} cell migration toward the ASML^{wt}-matrix. Anti-panCD44 and anti-CD44v6 also inhibited AS-v6 and AS-v4–7, but not AS cell migration. ASML-v6^{kd} and ASML-v4–7^{kd} cell migration toward the ASML^{wt}-matrix was not significantly inhibited by anti-panCD44, anti-α6β4, or anti-c-Met (Fig. 2*B*). These results indicated that the ASML^{wt}-matrix-initiated migration essentially depends on CD44v6, but also involves c-Met- and α6β4. To control this hypothesis, HA, LN5 and HGF were used as stimulus. Surprisingly, all three molecules promoted migration of ASML^{wt} cells, although not as efficiently as the ASML^{wt}-matrix. Only HGF, albeit weakly stimulated ASML-v4–7^{kd} cell migration (Fig. 2*C*). Comparable results were obtained with human pancreatic cancer lines differing in c-Met, α6β4, and CD44v6 expression. Capan2 cells (CD44v6$^+$/c-Met$^+$/α6β4$^+$) migrated in response to HA, LN5 and HGF. Inhibition of migration by anti-CD44v6, anti-c-Met, and anti-β4 was stimulus-independent. Even in the absence of c-Met (8.18 cells), anti-CD44v6, and anti-β4 inhibited migration, which was not promoted by HGF and not inhibited by anti-c-Met. HA, LN5, or HGF poorly stimulated migration of Pt45P1 cells (CD44v6$^-$/c-Met$^-$/α6β4$^\pm$), which was weakly inhibited by anti-β4 (supplemental Fig. S2).

Having demonstrated that rat and human tumor lines migrate toward HGF and LN5 only as far as they express the corresponding receptors plus CD44v6, we finally asked, whether the failure of ASML^{wt} cells to migrate toward the ASML-v4–7^{kd}-matrix relies exclusively on the low level of higher molecular weight HA. Addition of HA to the ASML-v4–7^{kd}-matrix hardly strengthened ASML^{wt} and not at all ASML-v4–7^{kd} cell migration (Fig. 2*D*). This indicates that the ASML-v4–7^{kd} matrix, by assembly or composition, actively inhibits tumor cell migration.

Thus, CD44v6-competent tumor cells can assemble a matrix that promotes migration, whereas in the absence of CD44v6, at least in ASML cells, a matrix is assembled that actively inhibits migration. Though less efficiently, migration can also be initiated by HA, HGF, and LN5. However, irrespective of the initiating stimulus, CD44v6 expression is essentially required as CD44v6-deficient cells do not or poorly respond to the migration-promoting stimuli.

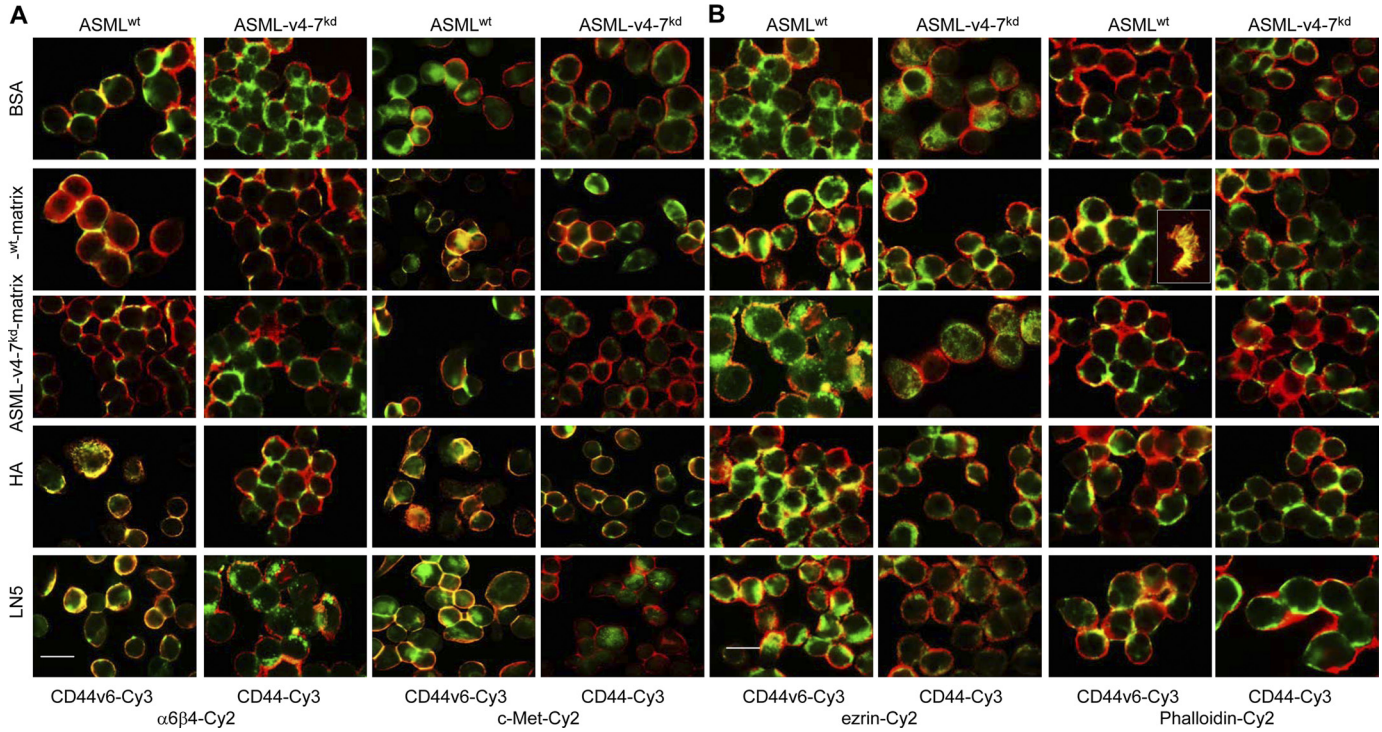

FIGURE 3. **The ASML^{wt} matrix supports co-localization of CD44v6 with $\alpha6\beta4$, c-Met, ezrin, and F-actin.** ASML^{wt} and ASML-v4–7^{kd} cells were seeded on HA, LN5, the ASML^{wt}-, or ASML-v4–7^{kd}-matrix and were stained with A2.6 or Ox50 plus (*A*) B5.5 and anti-c-Met or (*B*) anti-ezrin and phalloidin. *Inset*, membrane fragments, left behind (migrating) cells, have only been seen, when ASML^{wt} cells were seeded on the ASML^{wt}-matrix. Overlays of single fluorescence microscopy are shown (bar size: 5 μm). The ASML^{wt}-matrix, HA, and LN5, but not the ASML-v4–7^{kd}-matrix strengthen co-localization of CD44v6 with $\alpha6\beta4$, c-Met, ezrin, and F-actin.

CD44v6-dependent Motility Is Accompanied by c-Met, Ezrin, and Src Activation—Immunofluorescence of ASML^{wt} cells revealed pronounced co-localization of CD44v6 with $\alpha6\beta4$ and c-Met, when seeded on HA-, LN5-, ASML^{wt}-, but not ASML-v4–7^{kd}-matrix-coated slides. Instead, the CD44 standard molecule poorly co-localized with $\alpha6\beta4$ and c-Met in ASML-v4–7^{kd} cells (Fig. 3*A*). As CD44, upon activation, also associates via ezrin with the actin cytoskeleton, we evaluated CD44 co-localization with ezrin and F-actin, which was strong in ASML^{wt} cells, when seeded on HA-, LN5-, or ASML^{wt}-matrix-, but not ASML-v4–7^{kd}-matrix-coated slides. Co-localization was weak in ASML-v4–7^{kd} cells (Fig. 3*B*). FAK, which can become attracted via CD44-associated src, also preferentially co-localized with CD44v6 when ASML^{wt} cells were seeded on the ASML^{wt}-matrix or on LN5 (data not shown). The same observations accounted for CD44v6 co-localization with $\beta4$, ezrin, FAK, c-Met, and actin bundles in Capan2 cells. HA- and LN5 also stimulated, albeit less pronounced, co-localization of CD44v6 and $\beta4$ with actin bundles in 8.18 cells (supplemental Fig. S3).

Co-localization of c-Met with CD44v6 was accompanied by strong c-Met phosphorylation, when cells were stimulated by the ASML^{wt}-matrix, HA, LN5, or HGF. Instead, only weak c-Met phosphorylation was observed, when ASML-v4–7^{kd} cells were stimulated by the ASML^{wt}-matrix, or HGF, but not when stimulated with HA or LN5 (Fig. 4*A*). The finding not only confirms the impact of the ASML^{wt}-matrix on c-Met activation, but also strengthens the notion that irrespective of the initiating stimulus, c-Met activation is greatly facilitated by CD44v6. As demonstrated for HA cross-linking, ezrin phosphorylation is also strongly promoted by CD44v6 expression. In lysates of ASML^{wt}, AS-v6, or AS-v4–7 cells cultured on HA-coated plates, an increased amount of phosphorylated ezrin co-immunoprecipitated with CD44v6. However, HA-binding of CD44s in ASML-v4–7^{kd} or AS cells hardly strengthened co-immunoprecipitation of phosphorylated ezrin with CD44s (Fig. 4*B*).

In addition, FAK and src co-immunoprecipitation and phosphorylation became strengthened by CD44-crosslinking via HA (Fig. 4*C*). Src and FAK also became phosphorylated in HA-treated AS-v4–7, but not in ASML-v4–7^{kd} and AS cells. Furthermore, although src co-immunoprecipitated with CD44s and CD44v, p-src was only recovered in anti-CD44 precipitates of CD44v6-competent cells (Fig. 4*D*).

Taken together, migratory activity of CD44v6-competent tumor cells is accompanied by c-Met phosphorylation, recruitment, and phosphorylation of ezrin and pronounced phosphorylation of FAK via CD44-associated src. None of these observations are discerned for CD44v6-deficient cells. This confirms that transition toward the migratory phenotype, initiated via c-Met, $\alpha6\beta4$, or CD44v6 ligand binding, essentially requires CD44v6 for signal transduction downstream of c-Met, ezrin, and src. This central role of CD44v6 in signal transduction has also been seen in matrix-supported drug resistance.

Matrix-assisted Drug Resistance—ASML cells grow anchorage-independent with a soft agar cloning efficacy of close to 100%, which is not affected by the CD44v4–7^{kd} (43). They have a slow cell cycle, where the proliferative activity is not altered in ASML-v4–7^{kd} cells (43) and neither the ASML^{wt}- nor the ASML-v4–7^{kd}-matrix influence cell cycle progression of

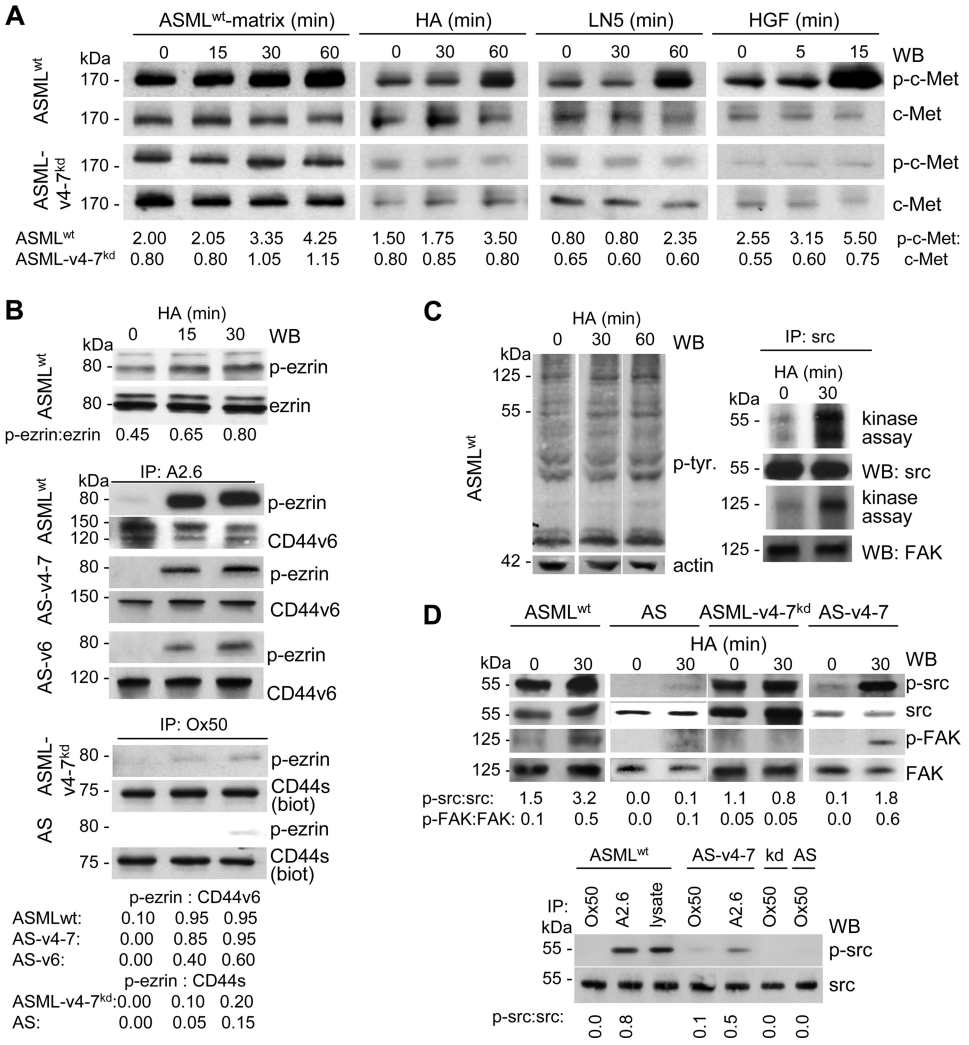

FIGURE 4. **CD44v6 dependence of c-Met, ezrin, src, and FAK activation.** *A*, ASML^{wt} and ASML-v4–7^{kd} cells were stimulated with ASML^{wt}-matrix, HA (10 μg/ml), LN5 (2 μg/ml), and HGF (5 ng/ml). Lysates (25 μg) were separated by SDS-PAGE and after protein transfer blotted with anti-p-c-Met and anti-c-Met. *B*, ASML^{wt} cells were stimulated with HA (10 μg/ml). Lysates (25 μg) were separated by SDS-PAGE and after protein transfer blotted with anti-p-ezrin or anti-ezrin or lysates of ASML^{wt}, AS-v6, AS-v4–7 cells were immunoprecipitated with A2.6 or lysates of biotinylated ASML-v4–7^{kd} and AS cells were immunoprecipitated with Ox50. After SDS-PAGE and protein transfer membranes were blotted with anti-p-ezrin and A2.6, respectively, streptavidin. *C*, untreated and HA-treated (10 μg/ml) ASML^{wt} cells were lysed separated by SDS-PAGE and after protein transfer blotted with anti-p-tyrosine and anti-actin or were immunoprecipitated with anti-src. Precipitates were labeled with [γ-^{32}P]ATP. Autoradiography and blotting after SDS-PAGE separation and transfer with anti-src and anti-FAK are shown. *D*, HA-treated ASML^{wt}, AS-v4–7, ASML-v4–7^{kd}, and AS cells were lysed and were blotted, after SDS-PAGE separation and transfer, with anti-p-src, -src, -p-FAK, and -FAK. Alternatively, lysates were immunoprecipitated with A2.6 or Ox50 and SDS-PAGE separated immunoprecipitates were blotted with anti-p-src and -src. *A*, *B*, and *D*, ratios of non-phosphorylated to phosphorylated protein or of precipitated to co-precipitated protein are included. The ASML^{wt}-matrix, HA, LN5, and HGF strengthen the CD44v6, c-Met, and $\alpha 6\beta 4$ association, which is accompanied by ezrin, src, and FAK association/phosphorylation only in CD44v6-competent cells.

ASML^{wt} and ASML-v4–7^{kd} cells (Fig. 5*A*). Instead, proliferation and mitochondrial respiratory activity of ASML-v4–7^{kd}, but not of ASML^{wt} cells is impaired after 48 h of culture in the presence of 2.5 μg/ml cisplatin. As in the absence of cisplatin, proliferative activity of ASML^{wt}, and ASML-v4–7^{kd} cells did not differ, this indicates that the high drug resistance of ASML^{wt} cells (43) may be affected by the CD44v4–7^{kd}. Notably, the ASML^{wt}-matrix obviously supports drug resistance of ASML^{wt}, but hardly of ASML-v4–7^{kd} cells. In the presence of the ASML^{wt}-matrix, proliferative and mitochondrial respiratory activity of ASML^{wt} cells was unimpaired by 5 μg/ml cisplatin, while in the absence of the ASML^{wt}-matrix proliferative activity was reduced by roughly 30%.The ASML-v4–7^{kd}-matrix hardly exerted any protective effect on ASML^{wt} cells and none on ASML-v4–7^{kd} cells (Fig. 5 *B* and *C*). To control that the ASML^{wt}-matrix indeed protects from apoptosis, the apoptosis rate of ASML^{wt} and ASML-v4–7^{kd} cells cultured for 48 h in the presence of increasing doses of cisplatin was evaluated by AnnexinV/PI staining. High apoptosis resistance of ASML^{wt} cells was further increased in the presence of the ASML^{wt}-matrix. The ASML-v4–7^{kd}-matrix exerted no effect. ASML-v4–7^{kd} cells were not protected from apoptosis by their own and only weakly by the ASML^{wt}-matrix. HGF also promoted apoptosis resistance. Protection by HA and LN5 was weaker, but reached a significant level in ASML^{wt} cells at high cisplatin concentrations (Fig. 5*D*).

These findings indicated that CD44v6 plays a central role in apoptosis protection and that particularly c-Met might support CD44v6-mediated apoptosis resistance. The latter assumption was controlled by a transient c-Met and $\beta 4$

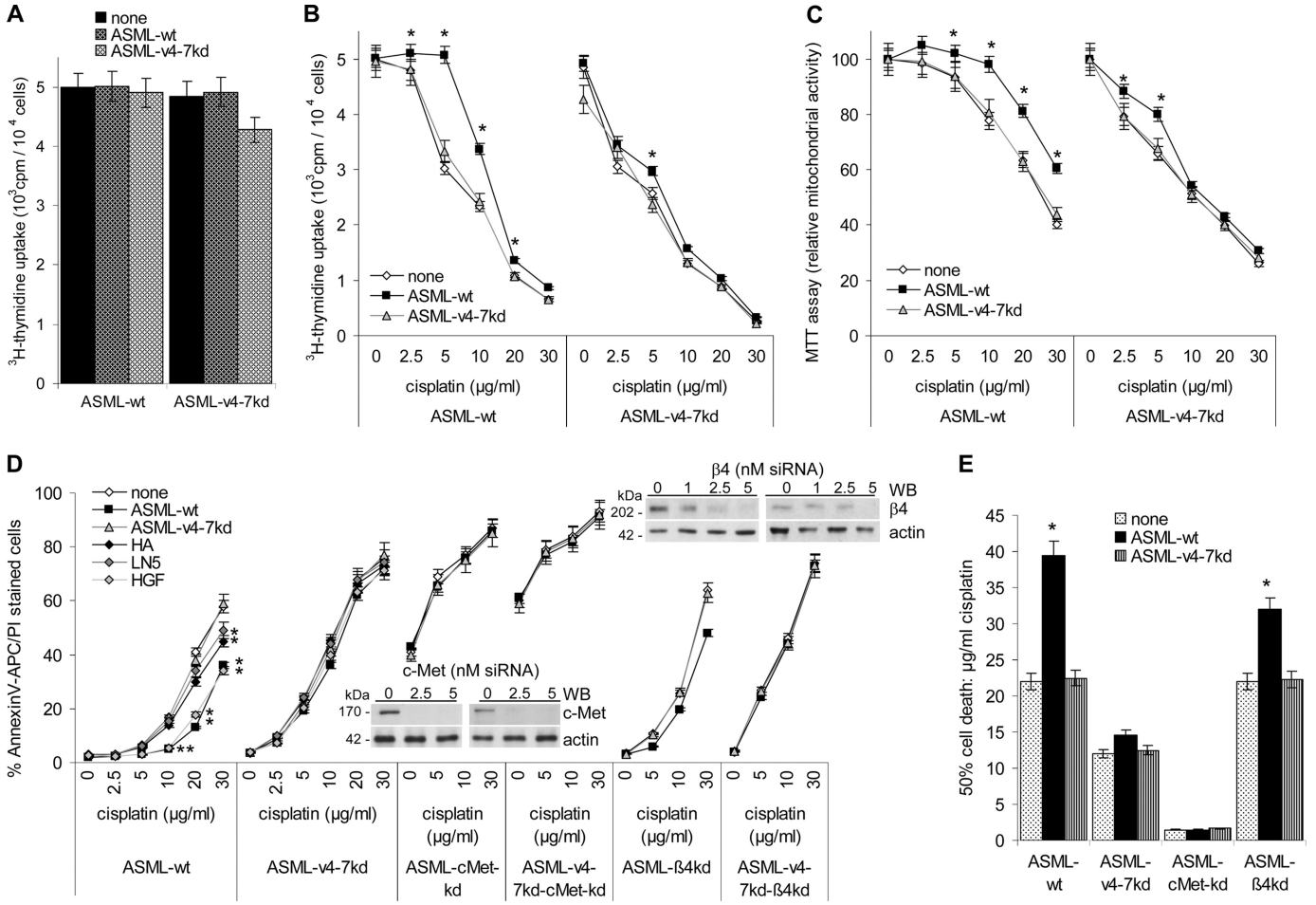

FIGURE 5. **The ASML^{wt}-matrix supports apoptosis resistance.** *A*, ASML^{wt} and ASML-v4–7^{kd} cells were seeded on BSA-, ASML^{wt}-matrix, or ASML-v4–7^{kd}-matrix and cultured for 48 h in the presence of RPMI/5%FCS containing [^{3}H]thymidine (10 μCi/ml). Mean + S.D. (triplicates) of [^{3}H]thymidine incorporation are shown. *B* and *C*, ASML^{wt} and ASML-v4–7^{kd} cells were seeded on BSA or ASML^{wt}-matrix- or ASML-v4–7^{kd}-matrix-coated plates and were cultured for 48 h in the presence of titrated amounts of cisplatin. Mean ± S.D. of triplicates of (*B*) proliferative activity ([^{3}H]thymidine incorporation) and (*C*) the relative mitochondrial respiratory activity (MTT assay) are shown. *D*, ASML^{wt} and ASML-v4–7^{kd} cells were seeded on BSA- or ASML^{wt}-matrix-, ASML-v4–7^{kd}-matrix-, HA-, LN5-, or HGF-coated plates; ASML^{wt}-cMet^{kd}, ASML-v4–7^{kd}-cMet^{kd}, ASML^{wt}-β4^{kd}, and ASML-v4–7^{kd}-β4^{kd} cells were seeded on BSA or ASML^{wt}-matrix- or ASML-v4–7^{kd}-matrix-coated plates. Cells were cultured for 48 h in the presence of titrated amounts of cisplatin. Mean ± S.D. of triplicates of the percentage of dead cells (AnnexinV-APC/PI staining) is shown. *Insets*, c-Met, β4, and, as control, actin WB after c-Met siRNA and β4-siRNA treatment. Mean ± S.D. of triplicates of the percentage of dead cells (AnnexinV-APC/PI staining) are shown. *E*, amount of cisplatin that is required to kill 50% of the indicated cells on uncoated or matrix coated plates is shown. *A–E*, significant differences between uncoated and coated plates are indicated by *. Proliferative activity of ASML cells is independent of CD44v6 and not supported by the ASML^{wt}-matrix. Instead, apoptosis resistance of ASML^{wt} and ASML-v4–7^{kd} cells essentially depends on c-Met expression and is supported by α6β4. The ASML^{wt}-matrix supports apoptosis resistance only in CD44v6-compentent cells.

knockdown. C-Met siRNA strongly affected ASML^{wt} and ASML-v4–7^{kd} viability even in the absence of cisplatin and the ASML^{wt} matrix did not exert a protective effect. Viability of ASML cells was not affected by the β4 knockdown. Nonetheless, the protective effect of the ASML^{wt}-matrix was weaker in ASML-β4^{kd} cells and was not seen in ASML-v4–7^{kd}-β4^{kd} cells (Fig. 5*E*). The contribution of the tumor matrix and the CD44v6-c-Met-α6β4 complex to apoptosis resistance was confirmed in Capan2, 8.18, and Pt45P1 cells. In the presence of the Capan2-matrix, proliferation, mitochondrial respiratory activity, and apoptosis were not affected by 7.5 μg/ml cisplatin. The Capan2-matrix also protected 8.18 cells (CD44v6$^+$, but c-Met$^-$), but hardly Pt45P1 cells (CD44v6$^-$, c-Met$^-$, α6β4$^\pm$). The Pt45P1-matrix was not protective, and the 8.18-matrix showed only minor protection on Capan2 and 8.18 cells (supplemental Fig. S4).

The impact of the matrix and of the CD44v6-c-Met-α6β4 complex on apoptosis resistance is summarized in Fig. 5*F*, which shows the dose of cisplatin that is required to kill 50% of the tumor cells. From there it becomes obvious that only the ASML^{wt}-, but not the ASML-v4–7^{kd}-matrix exerts a protective effect, when cells express, at least, CD44v6 and c-Met. Furthermore, c-Met exerts the strongest and α6β4 the weakest effect on apoptosis resistance. Finally, the partial rescue of apoptosis resistance by the ASML^{wt}-matrix in ASML^{wt}-β4^{kd}, but not in ASML-v4–7^{kd}-β4^{kd} cells is compatible with the interpretation that CD44v6 coordinates apoptosis-protecting signals delivered by c-Met and α6β4 (Fig. 5*F*).

CD44v6 Coordinates Activation of Anti-apoptotic Molecules—Activation of apoptosis-related signal transduction was evaluated in ASML^{wt} and ASML-v4–7^{kd} cells after stimulation with HA, HGF, and LN5.

Caspase-8 is the downstream caspase of death receptors. Caspase-8 activity increased in cisplatin-treated ASML^{wt} as well as ASML-v4–7^{kd} cells. This indicates that receptor-mediated apoptosis of ASML cells is not affected by the CD44v4–7^{kd}

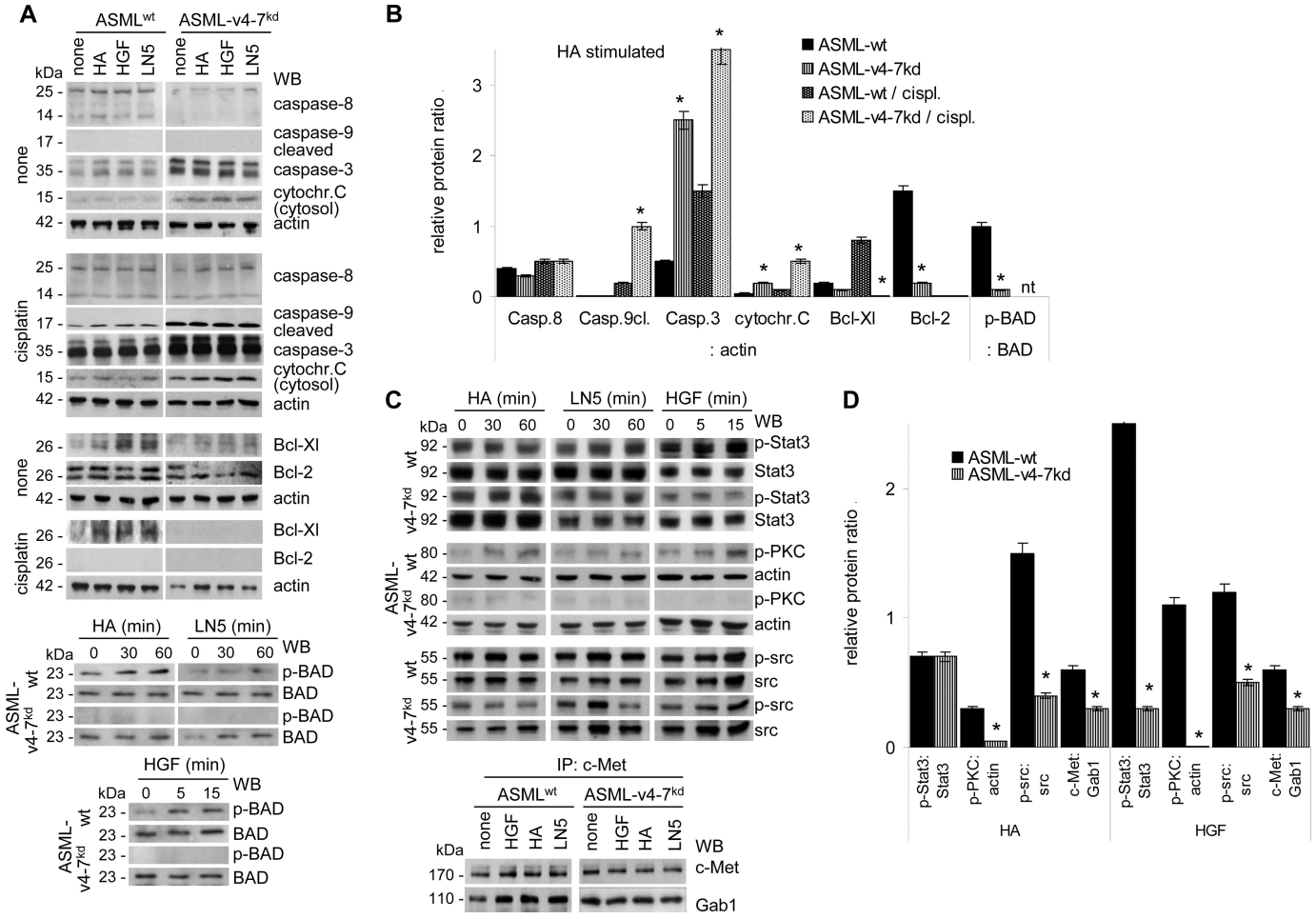

FIGURE 6. **The ASML^{wt}-matrix, HA, HGF, and LN5 promote up-regulation of anti-apoptotic proteins.** *A–D*, ASML^{wt} and ASML-v4–7^{kd} cells were stimulated with HA, LN5, and HGF as described above. *A*, where indicated, cells were cultured for 48 h in the presence or absence of 30 μg/ml cisplatin. Cells were lysed and, where indicated, the cytosolic fraction was isolated. WB anti-caspase-8, -caspase-9 (cleaved), -caspase-3, -cytochrome *c* (cytosolic fraction), -Bcl-Xl, -Bcl-2, -actin, BAD, and p-BAD; *B*, mean ± S.D. (3 experiments) of the band intensity ratio compared with actin or phosphorylated to non-phosphorylated protein is shown. Significant differences are indicated by *. *C*, WB anti-p-Stat3, -Stat3, -p-PKC, -actin, -p-src, -src, and WB with anti-c-Met and anti-Gab1 after IP with anti-c-Met. *D*, mean ± S.D. (three experiments) of the band intensity ratio of non-phosphorylated to phosphorylated protein or to actin is shown. Significant differences are indicated by *. Stimulation with HA, HGF, and LN5 is accompanied by reduced caspase-9 and caspase-3 activation, stabilization of mitochondrial membrane integrity, promotion of BAD phosphorylation, Bcl-2, and Bcl-Xl expression, strengthening of Stat3, PKC, and src phosphorylation and the association of c-Met with Gab1 indicating that CD44v6, c-Met, and $\alpha6\beta4$ jointly support apoptosis protection.

and that receptor-mediated apoptosis does not proceed through CD44v6, c-Met, or $\alpha6\beta4$.

On the contrary, caspase-9 cleavage and, less pronounced, caspase-3 expression was stronger in cisplatin-treated ASML-v4–7^{kd} than ASML^{wt} cells and higher amounts of cytochrome *c* were recovered in the cytosol. Thus, ASML^{wt} cells display more efficient protection toward the mitochondrial pathway of apoptosis than ASML-v4–7^{kd} cells, even though a protective effect of HA, LN5, or HGF was not observed after the prolonged culture period in the presence of cisplatin.

Reduced cytochrome *c* release and reduced caspases 9 and 3 activation in cisplatin-treated ASMLwt cells could be due to up-regulation of anti-apoptotic proteins. Indeed, Bcl-Xl and weakly Bcl-2 expression was increased in HA-, HGF-, and LN5-treated ASML^{wt}, but not ASML-v4–7^{kd} cells. Furthermore, Bcl-Xl expression remained up-regulated under cisplatin-treatment only in ASML^{wt} cells. Finally, in ASML^{wt}, but not in ASML-v4–7^{kd} cells, HA, LN5, and HGF supported phosphorylation of pro-apoptotic BAD, which allows for the release/functional activity of Bcl-2 and Bcl-Xl (Fig. 6*A*). Calculating the relative increase/decrease of these pro-and anti-apoptotic proteins in HA-stimulated untreated or cisplatin-treated ASML^{wt} *versus* ASML-v4–7^{kd} lysates revealed comparable activity of caspase-8 in both lines. This further supports that receptor-mediated apoptosis is CD44v6-independent. The relative increase of caspase-3, cleaved caspase-9 and cytosolic cytochrome *c* in cisplatin-treated ASML-v4–7^{kd} compared with ASML^{wt} cells confirms the higher apoptosis susceptibility of ASML-v4–7^{kd} cells to be due to the absence of CD44v6. This also accounts for the reduced recovery of the anti-apoptotic proteins Bcl-Xl and Bcl-2 as well as the reduced phosphorylation (inactivation) of BAD in HA-stimulated ASML-v4–7^{kd} compared with ASML^{wt} cells (Fig. 6*B*).

To further strengthen our hypothesis that in CD44v6-competent cells activation of signaling molecules via CD44 or c-Met or $\alpha6\beta4$ predominantly proceeds via CD44v6, we stimulated ASML^{wt} and ASML-v4–7^{kd} cells with HA, LN5, or HGF and evaluated activation of src, STAT3, and PKC, which are directly

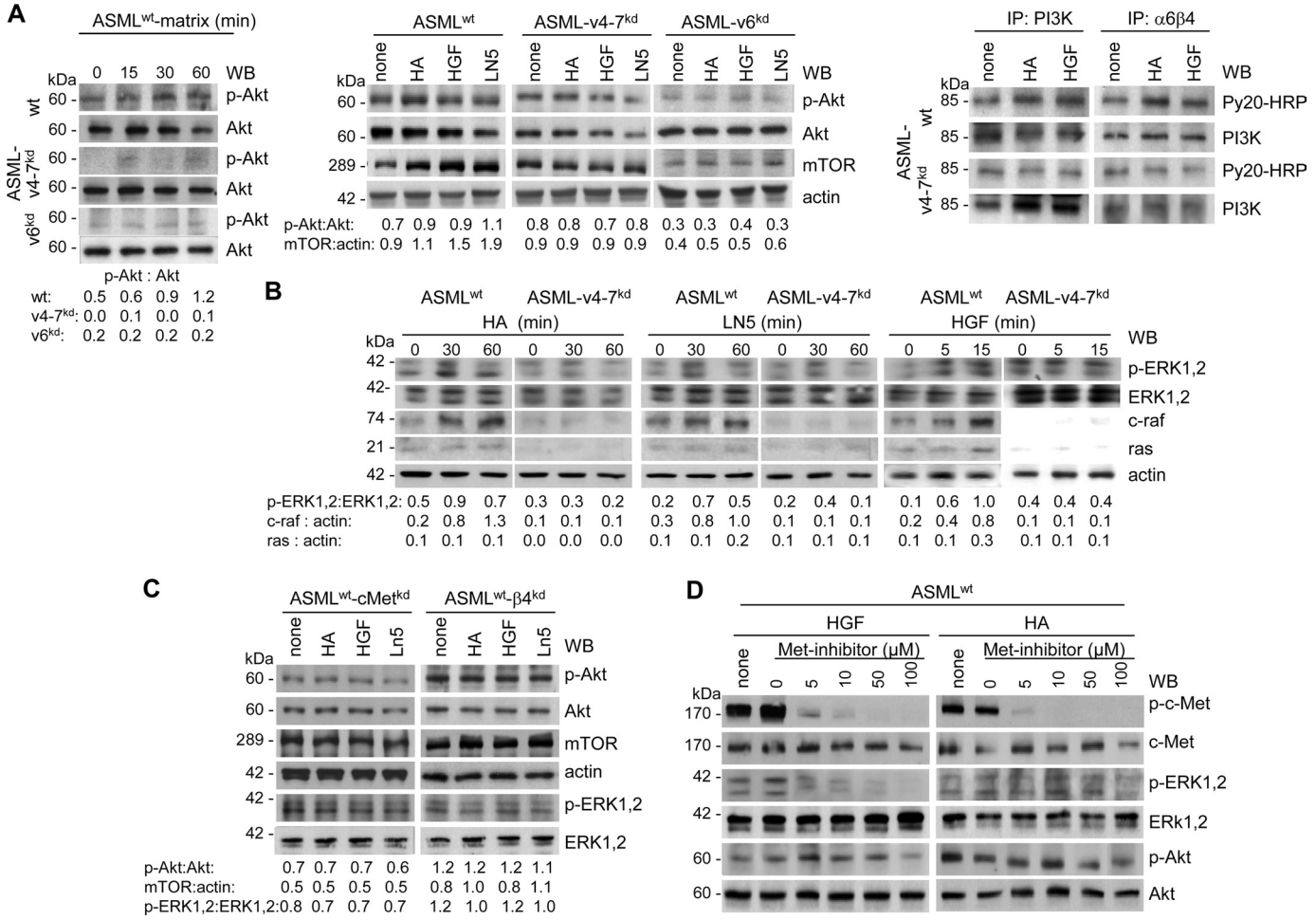

FIGURE 7. **The ASML^{wt}-matrix, HA, HGF, and LN5 initiate activation of the PI3K/Akt and the MAPK pathway.** *A* and *B*, ASML^{wt}, ASML-v4–7^{kd}, and ASML-v6^{kd} cells and (*C*) ASML^{wt}-cMet^{kd} and ASML^{wt}-β4^{kd} cells were stimulated with the ASML^{wt}-matrix, HA, LN5, and HGF as described above. Cells were lysed, and lysates were separated by SDS-PAGE and after transfer blotted with the indicated antibodies or (*A*, *right*) lysates were immunoprecipitated with anti-PI3K or B5.5 and immunoprecipitates, after SDS-PAGE and transfer, were blotted with anti-p-tyrosine and anti-PI3K. *A–C*, ratio of non-phosphorylated to phosphorylated protein or to actin is included. *D*, ASML^{wt} cells were stimulated with HGF or HA in the presence of the Met inhibitor SU11274. After lysis, SDS-PAGE and transfer, blots were incubated with the indicated antibodies. The ASML^{wt}-matrix, HA, HGF, and LN5 support activation of both the PI3K/Akt and the ras/raf/MAPK pathway. Selective inhibition of the MAPK pathway suggests, at least, a partly independent activation of the PI3K and the MAPK pathway.

associated with c-Met. Stat3 phosphorylation was most pronounced after HGF-cross-linking, but only in ASML^{wt} cells. PKC and src phosphorylation were equally well promoted by HA, LN5, and HGF in ASML^{wt}, but not ASML-v4–7^{kd} cells. Furthermore, HGF, HA, and LN5 promoted co-immunoprecipitation of c-Met with Gab1 more efficiently in ASML^{wt} than ASML-v4–7^{kd} cells (Fig. 6*C*). Calculating the ratio of the phosphorylated to non-phosphorylated proteins in ASML^{wt} and ASML-v4–7^{kd} cells confirmed that HGF and HA equally well supported PKC, src, and Gab1 phosphorylation, however, only in CD44v6-competent cells. STAT phosphorylation has been the only exception in as much as it was more strongly stimulated by HGF than HA. Nonetheless, the effect was not seen in CD44v-deficient cells (Fig. 6*D*). These findings imply that activation of anti-apoptotic proteins can be initiated via HGF or HA. But, activation of downstream signaling cascades is greatly facilitated by CD44v6.

Apoptosis Resistance Proceeds via the PI3K/Akt and MAPK Pathways—Apoptosis protection can be initiated by activation of the PI3K/Akt or the ras-raf-MAPK pathway. Akt phosphorylation and mTOR expression were up-regulated in ASML^{wt}-matrix, HA-, LN5-, and HGF-stimulated ASML^{wt}, but not ASML-v4–7^{kd} or ASML-v6^{kd} cells. Furthermore, a higher amount of phosphorylated PI3K was recovered in HA- or HGF-stimulated ASML^{wt} than ASML-v4–7^{kd} cells and p-PI3K co-immunoprecipitated with α6β4 (Fig. 7*A*). Ligand binding of CD44v6, c-Met, and α6β4 also sufficed for ras, c-raf, and ERK1,2 activation. Activation was not observed in the absence of CD44v6 (Fig. 7*B*).

To confirm a joint contribution of CD44v6, c-Met, and α6β4, the experiment was repeated with c-Met- and β4-siRNA-treated ASML cells. HA-, HGF-, and LN5-initiated ERK1,2 and Akt phosphorylation and mTOR up-regulation were strongly reduced after c-Met silencing. The β4-knockdown exerted a similar, though less pronounced effect (Fig. 7*C*). Finally, when ASML^{wt} cells were stimulated with HGF in the presence of the Met-inhibitor SU11274, c-Met, and ERK1,2 phosphorylation of ASML^{wt} cells was strongly reduced at 5 μM SU11274. However, 10 μM SU11274 did not affect Akt phosphorylation and a partial reduction was only seen with 100 μM

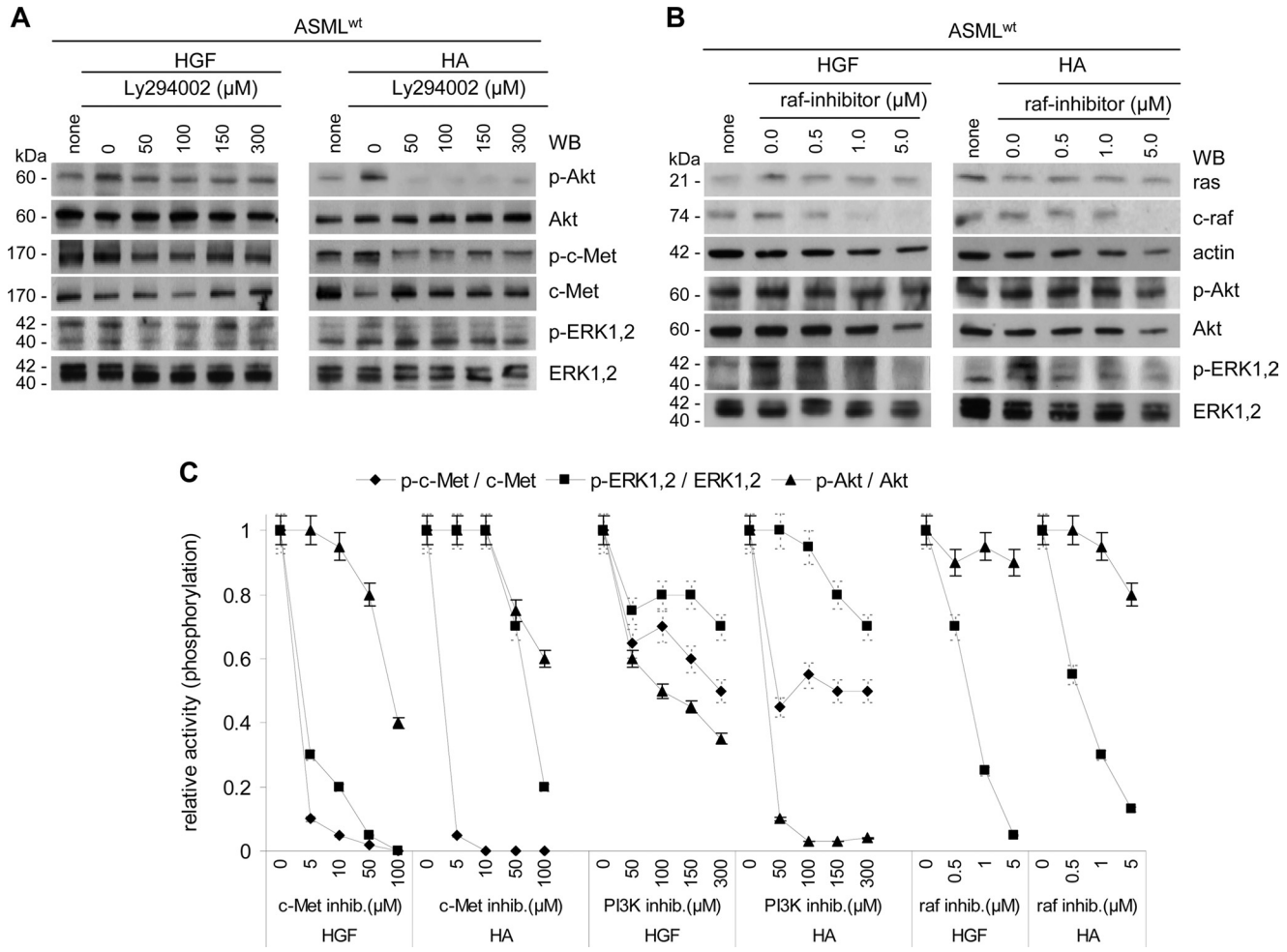

FIGURE 8. **Preferential activation of the MAPK pathway by HGF and of the PI3K/Akt pathway by HA.** *A* and *B*, ASML^{wt} cells were stimulated with HGF or HA in the presence of (*A*) the PI3K inhibitor Ly294002 or (*B*) the raf inhibitor GW5074. After lysis, SDS-PAGE and transfer, blots were incubated with the indicated antibodies. *C*, relative ratios of p-Akt:Akt, p-c-Met:c-Met, and p-ERK1,2:ERK1,2 (mean ± S.D. of three assays) depending on the stimulus and the inhibitor are shown. The ratio in the absence of an inhibitor has arbitrarily been taken as 1.0. Inhibition of c-Met and raf hardly affects Akt activation. Instead, activation of the MAPK pathway becomes only partially inhibited by a blockade of PI3K. These findings imply an independent activation of both pathways, despite the essential requirement of CD44v6 in activation of both.

SU11274. A similar inhibition profile was observed upon HA stimulation: SU11274 strongly inhibited c-Met and ERK1,2, but only partially Akt phosphorylation (Fig. 7*D*).

We interpret these findings to indicate that (i) both PI3K and MAPK pathway activation contribute to ASML^{wt}-matrix, HA-, LN5-, and HGF-initiated apoptosis resistance and (ii) anti-apoptotic signal transduction converges downstream of CD44v6. However, (iii) the weak effect of c-Met inhibition on Akt phosphorylation pointed toward independent activation of the MAPK and PI3K/Akt pathway.

To control for independent PI3K and MAPK pathway activation, ASML^{wt} cells were stimulated by HGF and HA in the presence of the PI3K-inhibitor Ly294002 or the raf-inhibitor GW5074. Akt inhibition was more pronounced in HA- than HGF-stimulated cells. Nonetheless, already 50 μM Ly294002 inhibited Akt phosphorylation in HA-stimulated ASML^{wt} cells. On the contrary, c-Met and ERK1,2 phosphorylation was less severely impaired (Fig. 8*A*). The raf-inhibitor (1 μM) strongly affected c-raf expression and ERK1,2 phosphorylation. Akt phosphorylation remained unaltered (Fig. 8*B*).

Thus, PI3K/Akt and ras-raf-MAPK pathway activation contribute to apoptosis resistance. Though activation of both pathways involves CD44v6 due to its association with c-Met and $\alpha6\beta4$, PI3K/Akt and MAPK pathway activation are not linked (Fig. 8*C*).

Taken together, ASML^{wt} cells secrete a matrix, whose composition is strongly influenced by CD44v6. The matrix, prone for storage of matrix-degrading enzymes and growth factors, facilitates migration via the association of ezrin and src/FAK with CD44, most pronounced CD44v6 and promotes apoptosis resistance via MAPK and PI3K/Akt pathway activation. Motility and apoptosis resistance can become initiated via CD44v6-HA, c-Met-HGF, and $\alpha6\beta4$-LN5 binding. Nonetheless, increased motility and apoptosis resistance in response to HGF, HA, and LN5 are only seen in CD44v6-competent cells (Fig. 9). Thus, activation of motility-promoting and apoptosis-protecting signals via c-Met and $\alpha6\beta4$ ligand binding are strongly supported by CD44v6.

DISCUSSION

Metastasizing tumor cells rely on a crosstalk with the environment, which at least in part, is supported by the tumor

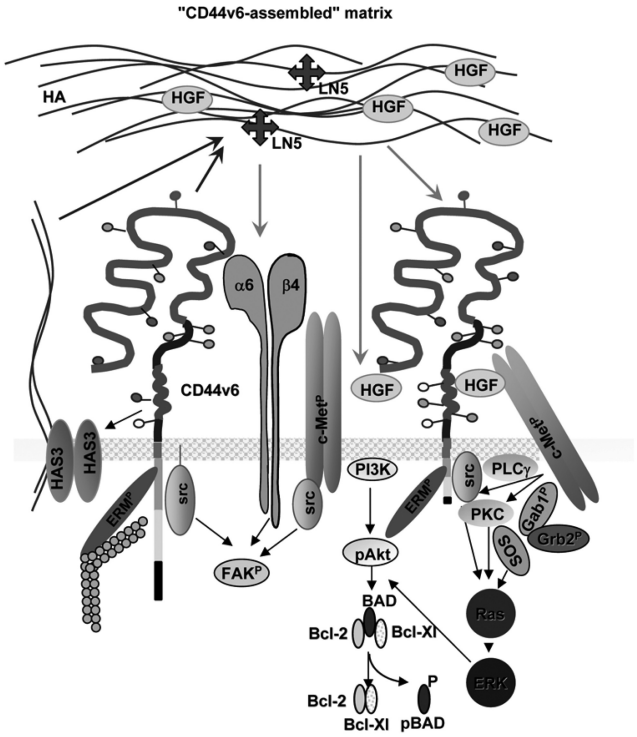

FIGURE 9. **Coordinating activity of CD44v6 in tumor matrix assembly and matrix assisted tumor cell motility and apoptosis resistance.** CD44v6 promotes by not yet defined mechanisms up-regulation of HAS3 with more abundant secretion of HMW HA. Besides others, this matrix is enriched in LN5 and HGF. By receptor binding HA, LN5, and HGF stimulate motility and apoptosis resistance. Both activities, motility and apoptosis resistance become significantly strengthened in cell expressing CD44v6. This is due to CD44v6 supporting c-Met activation by presenting HGF (27, 28) as well as by CD44v6 coordinating signals downstream of $\alpha6\beta4$ and c-Met as outlined in the scheme.

matrix (49). Furthermore, we recently reported that assembly of a metastasis-promoting matrix (44) was strikingly CD44v6-dependent and provided evidence for a feedback loop, such that the matrix strengthened tumor cell adhesiveness and drug resistance (43). We here explored the molecular mechanisms underlying this feedback cross-talk, which unexpectedly revealed that CD44v6 ligation/activation besides being an initial trigger, most efficiently coordinates signals initiated by c-Met and $\alpha6\beta4$ ligand binding.

CD44v6 and Matrix Assembly—In line with published evidence, HA-bound CD44 can contribute to c-Met, uPAR, and HAS3 transcription (50–52), expression of the three molecules being strongly reduced in ASML-v4–7^{kd} cells and the matrix (44). The increased level of HAS3, known to favor the malignant phenotype (53), in $ASML^{wt}$ cells corresponds to the higher amount and higher MW of HA in the $ASML^{wt}$- than the ASML-v4–7^{kd}-matrix. However, we do not yet know at what level CD44v6 expression regulates HAS3. Recovery of lower MW HA in the ASML-v4–7^{kd}-matrix is in line with the higher recovery of HAase, where we do not yet know the linkage between CD44v deficiency and HAase transcription or stabilization. However, it is known that HA functions vary considerably with length (54). Thus, pronounced HA degradation in the ASML-v4–7^{kd}-matrix might well contribute to its inefficacy compared with the $ASML^{wt}$-matrix. Nonetheless, it is not merely the reduction in high MW HA, which hampers functional activity of the ASML-v4–7^{kd}-matrix, as addition of HA to the ASML-v4–7^{kd}-matrix provides only a weak migratory stimulus for $ASML^{wt}$ and none for ASML-v4–7^{kd} cells. Taking this into account and the notion that HAase can also act as a tumor promoter (55), it becomes unlikely that only the higher level of HAase in the ASML-v4–7^{kd} matrix suffices to explain its inhibitory effect.

In fact, additional molecule recovery is strongly reduced in the ASML-v4–7^{kd}-matrix, although expression is largely unaltered in ASML-v4–7^{kd} cells. These include $\alpha6\beta4$, the proteases MMP2, MMP9, uPA, CD13, and 2 hrta serine peptidases, chaperons involved in removing improperly folded molecules (56). Reduced protease recovery in the ASML-v4–7^{kd}-matrix could well influence matrix assembly. Hepatoma-derived growth factor (HDGF), too, is more abundantly recovered in the $ASML^{wt}$- than the ASML-v4–7^{kd}-matrix. High level HDGF expression protects from apoptosis and is associated with poor survival of cancer patients (57). Vimentin, enolase-1, clusterin, ECM protein-1, and DJ-1 are also strongly enriched in the $ASML^{wt}$-matrix. Soluble clusterin, a prosurvival chaperon-like molecule, influences chemokine secretion and supports intercellular communication (58). ECM-1, which interacts with perlecan, fibulin-1C/D and MMP-9, interferes with angiogenesis (59). High level ECM-1 in the $ASML^{wt}$-matrix might explain the poor vascularization of ASML tumors (42). Potential activities of DJ-1, a negative regulator of PTEN (60) within the matrix are unknown. Loss of the anaphylatoxin C3a and the CD11b ligand C3b likely affect host cell recruitment (61).

Taken together, these multiple effects of a $CD44v^{kd}$ on protein delivery were unexpected and require further exploration. This implies that, at the present state of knowledge, we cannot speculate on a possible negative impact of the ASML-v4–7^{kd} matrix on either the tumor cell or the surrounding. However, the higher recovery of *e.g.* HA, HGF, MMPs, uPA, LN5, and others in the $ASML^{wt}$-matrix could well contribute to the crosstalk between the matrix and the tumor cells and allowed us to proceed toward unraveling the particular contribution of CD44v6.

The $ASML^{wt}$-matrix Supports Migration via CD44v6—A subfraction of the $ASML^{wt}$-matrix promotes $\beta1$-integrin-dependent, but CD44v6-independent tumor cell adhesion such that ASML-CD44v4–7^{kd} cells readily adhere to the $ASML^{wt}$-matrix (43). Instead, tumor cell migration toward the $ASML^{wt}$-matrix strikingly depends on CD44v6, as neither AS nor ASML-v4–7^{kd} nor ASML-$v6^{kd}$ cells receive a migratory stimulus from the $ASML^{wt}$-matrix. Nonetheless, $ASML^{wt}$ cell migration is equally well inhibited by anti-CD44v6, anti-$\alpha6\beta4$ and anti-c-Met. Conversely, HA, LN5, and HGF support $ASML^{wt}$, but not ASML-v4–7^{kd} cell migration. This has been a first hint that ligand interaction of CD44v, c-Met, and $\alpha6\beta4$ contributes to migration, but transition to the migratory phenotype is strongly promoted by CD44v6, where signaling converges due to the association of the three molecules (20, 28). Indeed, signal transduction can proceed, independent of the initiating stimulus, downstream of CD44v6 toward ERM binding and phosphorylation (28). In addition, CD44-associated src becomes phosphorylated, which is accompanied by FAK recruitment toward

CD44v6 and FAK phosphorylation. Phosphorylation of the β4 chain can contribute by binding of the PTB domain of shc, which is required for shc phosphorylation and recruitment of Grb/SOS (62). C-Met also binds shc and src, which leads to FAK activation and by Gab1 binding many signaling cascades, including the MAPK pathway, become activated (63).

Taken together, though not excluding a direct contribution by c-Met and α6β4 to matrix-initiated migration, our data convincingly demonstrate an essential contribution of CD44v6, as only CD44v6-competent, but not CD44v6-deficient human and rat pancreatic adenocarcinoma cells respond to HA, LN5, HGF and, importantly, the tumor cell natural surrounding, as far as the matrix is delivered by a CD44v6-competent cell. The contribution of CD44v6 relies on its association with c-Met and α6β4 and, beyond this, the coordination of signal transduction initiated through this complex.

Matrix-supported Drug Resistance and CD44v6-dependent MAPK and PI3K/Akt Pathway Activation—The $ASML^{wt}$-matrix protects only CD44v6-expressing cells from cisplatin-induced apoptosis. However, protection is abolished in $ASML^{wt}$-$cMet^{kd}$ and weakened in $ASML^{wt}$-$\beta4^{kd}$ cells. Receptor-mediated apoptosis is not involved, as caspase-8 activation does not differ in $ASML^{wt}$ *versus* ASML-v4–7^{kd} cells. Instead, caspase-9 activation and release of cytochrome *c* are stronger in cisplatin-treated ASML-v4–7^{kd} than $ASML^{wt}$ cells. In line with these findings, BAD phosphorylation and Bcl-Xl expression become strengthened by CD44v6, c-Met, and α6β4 activation in $ASML^{wt}$ cells. Only in $ASML^{wt}$ cells, phosphorylation of directly c-Met-associated Stat3 and src (64), which both also associate with CD44 (11), was particularly pronounced after c-Met triggering. PKC phosphorylation and the c-Met-Gab1 association was stimulated by HA, LN5, and HGF in $ASML^{wt}$ cells. Similar to matrix-assisted migration, drug-resistance depended on CD44v6-coordinated signal transduction as demonstrated for the PI3K/Akt and MAPK pathways.

Though CD44v6 contributed to both PI3K/Akt and MAPK activation, Akt phosphorylation was only slightly impaired, when cells were stimulated with HA or HGF in the presence of a c-Met or a raf inhibitor. On the other hand, ERK1,2 phosphorylation became only partly blocked by a PI3K-inhibitor, which efficiently interfered with Akt phosphorylation. Thus, the MAPK and PI3K/Akt pathways contribute independently to apoptosis resistance initiated by CD44v6 or c-Met ligand binding. Nonetheless, in line with the CD44v6-c-Met-α6β4 association (20, 27, 28, 65), pronounced activation of both pathways essentially requires CD44v6 and c-Met, deletion of either molecule being accompanied by impaired apoptosis resistance. The point of convergence of signals initiated via c-Met, α6β4, and CD44v6 remains to be defined. We expect and are currently exploring, whether joint signal transduction depends on complex assembly in tetraspanin-enriched membrane microdomains, known as docking sites for kinases and adaptor proteins (66). Our hypothesis is supported by the findings that tetraspanins associate with c-Met, CD44v, and α6β4 (67–69).

In the latter context, it also should be mentioned that induction of a migratory phenotype can be accompanied by increased apoptosis resistance (reviewed in Ref. 70). This notion is well in line with activation-induced recruitment of c-Met, CD44v, and α6β4 into tetraspanin-enriched membrane microdomains as well as the convergence of signal transduction downstream of CD44v6. Nonetheless, α6β4-LN5 binding more efficiently promoted migration than drug resistance. Furthermore, activation of anti-apoptotic proteins and inactivation of pro-apoptotic proteins independently proceeded through the MAPK and the PI3K/Akt pathway, though activation of both pathways is coordinated by CD44v6. Therefore, we consider it likely that transition toward a migratory phenotype and apoptosis resistance can, but must not essentially be linked, which may depend on cell furnishings with signal transduction molecules.

CD44v6 can essentially contribute to tumor progression. This, at least in part, is due to CD44v6 taking an essential role in assembling a tumor matrix that, beside others, is enriched in several proteases, high MW HA, HGF, and LN5. This matrix supports motility and apoptosis resistance, which is accompanied by ERM protein, src, FAK, c-Met, MAPK, and PI3K/Akt pathway activation via CD44v6 and CD44v6-associated c-Met and α6β4. These findings not only confirm the contribution of CD44v6 to c-Met and α6β4 activation, when stimulated with the separate ligands, but extends these findings to the natural surrounding of CD44v6-competent tumor cells. Beyond this, CD44v6 coordinates signals initiated via FAK, MAPK, and PI3K/Akt independent of whether or not CD44v6 has been directly engaged in the initial trigger. Thus, a soluble tumor matrix, whose assembly depends on CD44v6 forces the cross-talk with host tissue allowing for premetastatic niche preparation and triggers via CD44v6 metastasizing tumor cell migration and apoptosis resistance.

Acknowledgments—We thank Dr. C. Claas, Bioquant, University Heidelberg, for help with video microscopy, Dr. T. Kempf, Proteomic-Core-Facility, German Cancer Research Center, Heidelberg, for MALDI-TOF/PSDF analysis and Dr. T. S. Johnson for language corrections.

REFERENCES

1. Kopfstein, L., and Christofori, G. (2006) *Cell Mot. Life Sci.* **63,** 449–468
2. Nie, D. (2010) *Frontier Biosciences* **2,** 184–193
3. Stern, R. (2008) *Semin. Cancer Biol.* **18,** 238–243
4. Tsuji, T., Ibaragi, S., and Hu, G. F. (2009) *Cancer Res.* **69,** 7135–7139
5. Naor, D., Wallach-Dayan, S. B., Zahalka, M. A., and Sionov, R. V. (2008) *Semin. Cancer Biol.* **18,** 260–267
6. Marhaba, R., and Zöller, M. (2004) *J. Mol. Histol.* **35,** 211–231
7. Günthert, U., Hofmann, M., Rudy, W., Reber, S., Zöller, M., Haussmann, I., Matzku, S., Wenzel, A., Ponta, H., and Herrlich, P. (1991) *Cell* **65,** 13–24
8. Ponta, H., Sherman, L., and Herrlich, P. A. (2003) *Nat. Rev. Mol. Cell Biol.* **4,** 33–45
9. Aruffo, A., Stamenkovic, I., Melnick, M., Underhill, C. B., and Seed, B. (1990) *Cell* **61,** 1303–1313
10. Toole, B. P. (2004) *Nat Rev Cancer* **4,** 528–539
11. Bourguignon, L. Y., Zhu, H., Shao, L., and Chen, Y. W. (2001) *J. Biol. Chem.* **276,** 7327–7336
12. Tsukita, S., Yonemura, S., and Tsukita, S. (1997) *Trends Biochem. Sci* **22,** 53–58
13. Lamontagne, C. A., and Grandbois, M. (2008) *Exp. Cell Res.* **314,** 227–236
14. Yu, Q., and Stamenkovic, I. (2004) *Clin Exp Metastasis* **21,** 235–242
15. Lesley, J., English, N. M., Gál, I., Mikecz, K., Day, A. J., and Hyman, R. (2002) *J. Biol. Chem.* **277,** 26600–26608
16. Mohamadzadeh, M., DeGrendele, H., Arizpe, H., Estess, P., and Siegel-

man, M. (1998) *J. Clin. Invest.* **101,** 97–108
17. Corso, S., Comoglio, P. M., and Giordano, S. (2005) *Trends Mol Med* **11,** 284–292
18. Fjeldstad, K., and Kolset, S. O. (2005) *Curr. Drug Targets* **6,** 665–682
19. Taylor, K. R., and Gallo, R. L. (2006) *FASEB J.* **20,** 9–22
20. Bertotti, A., and Comoglio, P. M. (2003) *Trends Biochem. Sci* **28,** 527–533
21. Boccaccio, C., Andò, M., Tamagnone, L., Bardelli, A., Michieli, P., Battistini, C., and Comoglio, P. M. (1998) *Nature* **391,** 285–288
22. Bourguignon, L. Y., Gilad, E., and Peyrollier, K. (2007) *J. Biol. Chem.* **282,** 19426–19441
23. Sherman, L., Wainwright, D., Ponta, H., and Herrlich, P. (1998) *Genes Dev.* **12,** 1058–1071
24. Ghatak, S., Misra, S., and Toole, B. P. (2005) *J. Biol. Chem.* **280,** 8875–8883
25. Bourguignon, L. Y. (2001) *J. Mammary Gland Biol. Neoplasia* **6,** 287–297
26. Lynch, C. C., Vargo-Gogola, T., Martin, M. D., Fingleton, B., Crawford, H. C., and Matrisian, L. M. (2007) *Cancer Res.* **67,** 6760–6767
27. Orian-Rousseau, V., Chen, L., Sleeman, J. P., Herrlich, P., and Ponta, H. (2002) *Genes Dev.* **16,** 3074–3086
28. Orian-Rousseau, V., Morrison, H., Matzke, A., Kastilan, T., Pace, G., Herrlich, P., and Ponta, H. (2007) *Mol. Biol. Cell* **18,** 76–83
29. Föger, N., Marhaba, R., and Zöller, M. (2000) *Eur. J. Immunol.* **30,** 2888–2899
30. Ingley, E. (2008) *Biochim. Biophys. Acta* **1784,** 56–65
31. Girish, K. S., and Kemparaju, K. (2007) *Life Sci.* **80,** 1921–1943
32. Turley, E. A., Noble, P. W., and Bourguignon, L. Y. (2002) *J. Biol. Chem.* **277,** 4589–4592
33. Knudson, C. B., and Knudson, W. (2004) *Clin. Orthop. Relat. Res.* **427,** (suppl.), S152–S162
34. Hill, A., McFarlane, S., Johnston, P. G., and Waugh, D. J. (2006) *Cancer Lett.* **237,** 1–9
35. Kuhn, N. Z., and Tuan, R. S. (2010) *J. Cell. Physiol.* **222,** 268–277
36. Wang, N., Tytell, J. D., and Ingber, D. E. (2009) *Nat. Rev. Mol. Cell Biol.* **10,** 75–82
37. Couchman, J. R. (2010) *Annu. Rev. Cell Dev. Biol.* **26,** 89–114
38. Bennett, K. L., Jackson, D. G., Simon, J. C., Tanczos, E., Peach, R., Modrell, B., Stamenkovic, I., Plowman, G., and Aruffo, A. (1995) *J. Cell Biol.* **128,** 687–698
39. Wai, P. Y., and Kuo, P. C. (2008) *Cancer Metastasis Rev.* **27,** 103–118
40. Berdiaki, A., Nikitovic, D., Tsatsakis, A., Katonis, P., Karamanos, N. K., and Tzanakakis, G. N. (2009) *Biochim. Biophys. Acta* **1790,** 1258–1265
41. van der Voort, R. Taher, T. E., Wielenga, V. J., Spaargaren, M., Prevo, R., Smit, L., David, G., Hartmann, G., Gherardi, E., and Pals, S. T. (1999) *J. Biol. Chem.* **274,** 6499–6506
42. Matzku, S., Komitowski, D., Mildenberger, M., and Zöller, M. (1983) *Invasion Metastasis* **3,** 109–123
43. Klingbeil, P., Marhaba, R., Jung, T., Kirmse, R., Ludwig, T., and Zöller, M. (2009) *Mol. Cancer Res.* **7,** 168–179
44. Jung, T., Castellana, D., Klingbeil, P., Cuesta Hernández, I., Vitacolonna, M., Orlicky, D. J., Roffler, S. R., Brodt, P., and Zöller, M. (2009) *Neoplasia* **11,** 1093–1105
45. Rudy, W., Hofmann, M., Schwartz-Albiez, R., Zöller, M., Heider, K. H., Ponta, H., and Herrlich, P. (1993) *Cancer Res.* **53,** 1262–1268
46. Gobom, J., Schuerenberg, M., Mueller, M., Theiss, D., Lehrach, H., and Nordhoff, E. (2001) *Anal. Chem.* **73,** 434–438
47. Stern, M., and Stern, R. (1992) *Matrix* **12,** 397–403
48. Trusolino, L., Bertotti, A., and Comoglio, P. M. (2001) *Cell* **107,** 643–654
49. De Wever, O., and Mareel, M. (2003) *J. Pathol.* **200,** 429–447
50. Kobayashi, H., Suzuki, M., Kanayama, N., Nishida, T., Takigawa, M., and Terao, T. (2002) *Int. J. Cancer* **102,** 379–389
51. Comoglio, P. M., Giordano, S., and Trusolino, L. (2008) *Nat. Rev. Drug Discov.* **7,** 504–516
52. Lee, K. H., Choi, E. Y., Hyun, M. S., Jang, B. I., Kim, T. N., Lee, H. J., Eun, J. Y., Kim, H. G., Yoon, S. S., Lee, D. S., Kim, J. H., and Kim, J. R. (2008) *Clin. Exp. Metastasis* **25,** 89–96
53. Adamia, S., Maxwell, C. A., and Pilarski, L. M. (2005) *Curr. Drug Targets Cardiovasc. Haematol. Disord.* **5,** 3–14
54. Stern, R., Asari, A. A., and Sugahara, K. N. (2006) *Eur J. Cell Biol.* **85,** 699–715
55. Stern, R., and Jedrzejas, M. J. (2006) *Chem. Rev.* **106,** 818–839
56. Clausen, T., Southan, C., and Ehrmann, M. (2002) *Mol. Cell* **10,** 443–455
57. Tsang, T. Y., Tang, W. Y., Tsang, W. P., Co, N. N., Kong, S. K., and Kwok, T. T. (2008) *Apoptosis* **13,** 1135–1147
58. Pucci, S., Mazzarelli, P., Nucci, C., Ricci, F., and Spagnoli, L. G. (2009) *Adv. Cancer Res.* **105,** 93–113
59. Sercu, S., Zhang, L., and Merregaert, J. (2008) *Cancer Invest.* **26,** 375–384
60. da Costa, C. A. (2007) *Curr. Mol. Med.* **7,** 650–657
61. Erler, J. T., Bennewith, K. L., Cox, T. R., Lang, G., Bird, D., Koong, A., Le, Q. T., and Giaccia, A. J. (2009) *Cancer Cell* **15,** 35–44
62. Dans, M., Gagnoux-Palacios, L., Blaikie, P., Klein, S., Mariotti, A., and Giancotti, F. G. (2001) *J. Biol. Chem.* **276,** 1494–1502
63. Benvenuti, S., and Comoglio, P. M. (2007) *J. Cell. Physiol.* **213,** 316–325
64. Boccaccio, C., and Comoglio, P. M. (2006) *Nat Rev Cancer* **6,** 637–645
65. Klosek, S. K., Nakashiro, K., Hara, S., Goda, H., Hasegawa, H., and Hamakawa, H. (2009) *Biochem. Biophys. Res. Commun.* **379,** 1097–1100
66. Lingwood, D., and Simons, K. (2010) *Science* **327,** 46–50
67. Hemler, M. E. (2005) *Nat. Rev. Mol. Cell Biol.* **610,** 801–811
68. Yáñez-Mó, M., Barreiro, O., Gordon-Alonso, M., Sala-Valdés, M., and Sánchez-Madrid, F. (2009) *Trends Cell Biol.* **19,** 434–446
69. Zöller, M. (2009) *Nat. Rev. Cancer* **9,** 40–55
70. Lefranc, F., Brotchi, J., and Kiss, R. (2005) *J. Clin. Oncol.* **23,** 2411–2422